RAPID COMMUNICATIONS

PHYSICAL REVIEW B VOLUME 36, NUMBER 10 1 OCTOBER 1987

Far-infrared composite-medium study of sintered La_2NiO_4 and $La_{1.85}Sr_{0.15}CuO_{4-y}$

P. E. Sulewski, T. W. Noh, J. T. McWhirter, and A. J. Sievers
Laboratory of Atomic and Solid State Physics and Materials Science Center,
Cornell University, Ithaca, New York 14853-2501

(Received 14 July 1987)

The infrared and far-infrared properties of sintered La_2NiO_4 and $La_{1.85}Sr_{0.15}CuO_{4-y}$ are modeled accurately within the effective-medium approximation. The electrodynamic properties of $La_{1.85}Sr_{0.15}CuO_{4-y}$ grains are highly anisotropic with the strong 0.5-eV electronic transition polarized along the low-conductivity crystal direction. The apparent superconducting gap frequency for the sintered material depends crucially on the grain geometry. Our experimental data are fit with needlelike crystallites and $2\Delta/k_BT_c = 2.6$.

With the observation[1] in the far-infrared (FIR) reflectivity of anisotropy in the optical conductivity of single-crystal La_2NiO_4, a compound structurally isomorphic to $La_{1.85}Sr_{0.15}CuO_{4-y}$, a realistic effective-medium modeling of the optical data for both the superconducting and normal state of the sintered material becomes practical for the first time. Here it is shown that the effective-medium approximation[2] (EMA) applied to nonspherical grains with Lorentz oscillator contributions for the phonons and a two-dimensional (2D) Drude free-carrier conductivity provides a good description of the reflectivity of La_2NiO_4 and also the optical conductivity of $La_{1.85}Sr_{0.15}CuO_{4-y}$ obtained from a Kramers-Kronig analysis of the reflectivity measured on sintered samples. By modeling the effective conductivity in the superconducting state with the Mattis-Bardeen equations[3] in the EMA, we find a strong dependence on the grain geometry of both the apparent gap frequency and the magnitude of the excess absorptivity in the superconducting state above the gap.

Figure 1(a) shows a fit of the room-temperature data of Bassat *et al.*[1] in the FIR to the standard dielectric function model,[4]

$$\epsilon_a = \epsilon_{\infty,a}\prod_j \frac{\Omega_{ja\mathrm{LO}}^2 - \omega^2 - i\gamma_{ja}(\omega)}{\Omega_{ja\mathrm{TO}}^2 - \omega^2 - i\gamma_{ja}\omega} - \frac{\Omega_{pa}^2}{\omega(\omega + i\gamma_{pa})} , \quad (1)$$

where a indicates the crystal axis, and with the parameters recorded in Table I. The dotted curve is for light polarized with $\mathbf{E}\parallel\mathbf{c}$ and the dashed curve is for $\mathbf{E}\perp\mathbf{c}$. The crystal exhibits conductivity in the **a**-**b** plane and insulating behavior along the **c** direction.

The reflectivity of a polycrystalline composite[5] of La_2NiO_4 is shown by the open circles in Fig. 1(b). Knowing the complete conductivity spectrum produced by free carriers and phonons in the single crystal, we can proceed with the EMA in an attempt to reproduce the polycrystalline data.

The EMA has been applied to a single-component polycrystalline material with an anisotropic conductivity tensor, with the crystal symmetry axes randomly oriented for each spherical grain.[6] Since, for La_2NiO_4, the **a** and **b** axes are equivalent, the EMA equation has a relatively simple form, with a fixed fill fraction of $f = \frac{2}{3}$ for the metallic (i.e., in the **a** and **b** directions) component. If in addition the crystallites are allowed to be spheroids with the same symmetry as the conductivity tensor, then a single parameter, the depolarization factor L_c, along the **c** direction of the crystallite specifies this EMA. The effective conductivity is obtained by solving the following equation:

$$\frac{2}{3}\frac{\sigma_{ab} - \sigma_e}{(1 + L_c)\sigma_e + (1 - L_c)\sigma_{ab}} + \frac{1}{3}\frac{\sigma_c - \sigma_e}{2[(1 - L_c)\sigma_e + L_c\sigma_c]} = 0 . \quad (2)$$

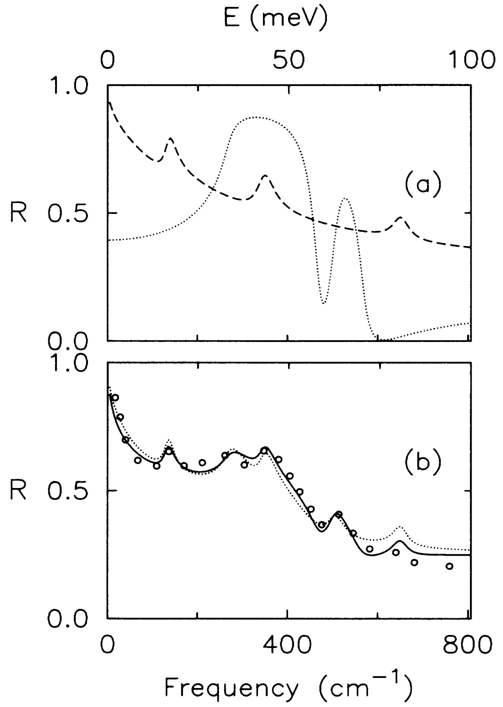

FIG. 1. Normal incidence reflectivity of La_2NiO_4 vs frequency. (a) Fits to single-crystal reflectivity of Bassat, Odier, and Gervais (Ref. 1) for light polarized with $\mathbf{E}\parallel\mathbf{c}$ (dotted curve) and $\mathbf{E}\perp\mathbf{c}$ (dashed curve). (b) Curves calculated with parameters in Table I from fits in (a) in EMA with $L_c = \frac{1}{3}$ (dotted line) and $L_c = 0.7$ (solid line). Data (open circles) for polycrystalline La_2NiO_4 of Gervais, Odier, and Nigara (Ref. 5).

TABLE I. Classical oscillator parameters used to fit La_2NiO_4 (Ni) and $La_{1.85}Sr_{0.15}CuO_{4-y}$ (Cu) reflectivity data.

		ω_{TO} (cm^{-1})	ω_{LO} (cm^{-1})	γ (cm^{-1})	ϵ_∞	ω_p (eV)	Γ (eV)
	(a,b)	135	180	17			
		345	380	30			
		649	662	35			
Ni					10.4	1.5	2.4
	(c)	270	470	30			
		502	570	28			
					4.9		
	(a,b)	135	150	20			
		360	390	30			
		650	660	35			
Cu					1.0	1.7	3.0
	(c)	242	465	45			
		494	595	20			
					35		

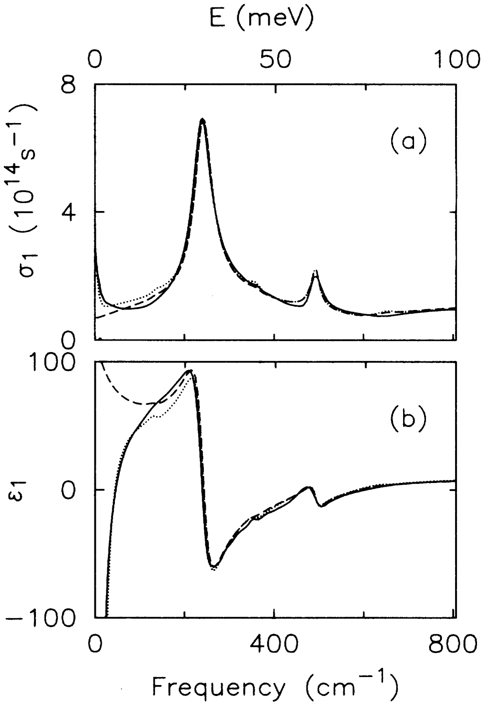

FIG. 2. Effective optical parameters vs frequency for sintered $La_{1.85}Sr_{0.15}CuO_{4-y}$. (a) Real part of the conductivity. (b) Real part of the dielectric function. Results obtained from a Kramers-Kronig analysis of the reflectivity (solid curve) compared with the EMA calculations (dashed curve) and also to a related model with a frequency dependent scattering rate for conduction electrons (dotted curve).

For the case of spherical crystallites, $L_c = \frac{1}{3}$ and Eq. (2) reduces to the standard result for an anisotropic polycrystalline material.[6] For needlelike crystallites $L_c = 0$ along the **c** axis, while for platelike crystallites $L_c = 1$.

The two curves shown in Fig. 1(b) result from the EMA by varying the depolarization factor L_c. The dotted curve is calculated with the assumption of spherical crystallites ($L_c = \frac{1}{3}$). The solid curve, which gives a slightly better fit to the data, corresponds to platelike crystallites ($L_c = 0.7$). The success of the fit is encouraging and lends credence to our next assumption.

Since La_2NiO_4 is isostructural to the superconducting compound $La_{1.85}Sr_{0.15}CuO_{4-y}$, we hypothesize the same extreme anisotropy of the conductivity and so again the observed reflectivity spectrum for the sintered sample should be described by an EMA which takes into account the anisotropy of the conductivity tensor. We have obtained the real and imaginary parts of the composite optical conductivity for the normal state from a Kramers-Kronig analysis of our reflectivity data which extends from 0.5 meV to 5 eV. The solid curves in Figs. 2(a) and 2(b) represent the experimental data in the far-infrared region. By taking basically the *same* phonon frequencies and strengths as for La_2NiO_4 and slightly changing the damping and the magnitude of the 2D conductivity (see Table I), we have been able to reproduce the qualitative features of the measured optical parameters for the sintered material down to about 150 cm^{-1}, as shown by the dashed curves in Figs. 2(a) and 2(b). We have used $L_c = 0.056$ to produce these curves, which corresponds to needlelike crystallites with an aspect ratio of 5.

Inspection of Table I shows that there is only one important difference between the normal-state parameters of the two materials and that is in the values of the dc dielectric contributions, ϵ_∞, from the electronic degrees of freedom along the different axes. In particular, $\epsilon_{\infty,c} = 35$ implies the existence of a low-lying interband transition in the **c** direction with a strength about twice that of Ge. Although not shown in Fig. 2, we do observe such an absorption band at 0.5 eV, and because of the large contribution to $\epsilon_{\infty,c}$ we assign the strong band exclusively to the **c** direction.

Figure 3(a) presents our FIR data on the reflectivity of $La_{1.85}Sr_{0.15}CuO_{4-y}$ in the normal state ($T = 40$ K, dashed curve) and in the superconducting state ($T = 10$ K, solid curve). The dashed line fit shown in Fig. 3(b) demonstrates that the Drude term does not provide enough reflectivity at low frequencies. The calculated reflectivity for the superconducting state represented by the solid line in Fig. 3(b) makes use of the Mattis-Bardeen equations[3] to model the 2D superconductivity in the **a**,**b** plane. This too reproduces some of the qualitative features observed in Fig. 3(a), for example, although 2Δ is chosen as 68 cm^{-1}, the onset of absorption occurs at about 35 cm^{-1}. Also, the reflectivities cross at 73.7 cm^{-1} and the normal state becomes more reflecting than the superconducting state above this frequency.

To demonstrate the key role of grain geometry, Fig. 3(c) shows the reflectivity in the superconducting and normal states as calculated with the EMA using identical parameters as Fig. 3(b), except that $L_c = 0.7$, corresponding to oblate spheroids. Immediately obvious is the dramatic loss of the enhanced absorptivity in the superconducting state above the gap and the shift in position of the equal reflectivity frequency, which in the past has been associat-

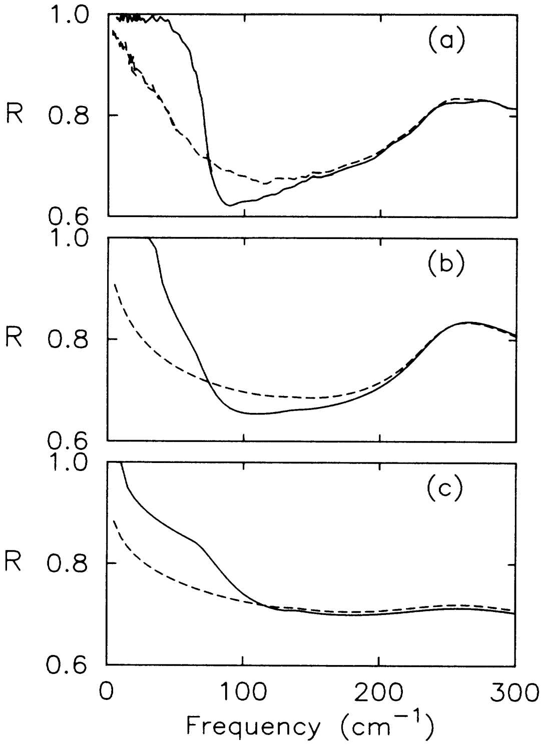

FIG. 3. Normal incidence reflectivity of sintered $La_{1.85}Sr_{0.15}CuO_{4-y}$ in the far infrared, in the superconducting (solid curves), and normal (dashed) states. (a) Measured reflectivity. (b) As modeled by the EMA with Mattis-Bardeen theory using $2\Delta/k_BT_c=2.6$, the parameters in Table I, and a depolarization factor $L_c=0.056$ (grains are prolate spheroids). (c) Same as (b), but with $L_c=0.7$ (oblate spheroids).

ed with the frequency of the energy gap 2Δ.

The large excess absorptivity in the superconducting state[7-9] and the apparent gap frequency observed in Fig. 3(a) are then due in part to the composite nature of the samples, which effectively couples the extremely large value of the dielectric function in the **c** direction to the **a**-**b** plane through the EMA. By analogy, we propose that the absence of enhanced absorptivity in the superconducting state above the apparent gap[10-12] in sintered $YBa_2Cu_3O_{7-y}$ may be a straightforward consequence of a different grain geometry.

The large difference between the low-frequency experimental data (solid lines) for σ_1 and ϵ_1 and the prediction of the classical oscillator model (dashed lines) shown in Fig. 2 has been accounted for by allowing the 2D carriers to respond with a frequency-dependent relaxation time.[13] Our particular phenomenological equations have been chosen to give a relaxation rate, which varies linearly with frequency at low frequencies, so that the effective carrier mass shows a logarithmic singularity at zero frequency, forms which are compatible with the recent proposal of Lee and Read.[14] The relaxation rate is

$$\Gamma(\omega)=\Gamma_{dc}+\frac{\lambda_0\omega}{(1+\omega^2a^2)^{1/2}}\ , \tag{3}$$

and the corresponding mass enhancement is

$$\lambda(\omega)=\frac{\lambda_0}{\pi(1+\omega^2a^2)^{1/2}}\ln\left[\frac{(1+\omega^2a^2)^{1/2}+1}{(1+\omega^2a^2)^{1/2}-1}\right]\ , \tag{4}$$

where Γ_{dc} is the magnitude of the frequency-independent scattering component and λ_0 and a^{-1} characterize the strength and the roll off, respectively, of the frequency dependent contribution. The dotted line fit to the data in Fig. 2 is obtained with $\Gamma_{dc}=400\ cm^{-1}$ (a value consistent with the dc resistivity), $\lambda_0=340$, $a^{-1}=70\ cm^{-1}$, $\epsilon_{\infty,ab}=3$, and all other parameters in Table I unchanged.

As yet, the analogs of the Mattis-Bardeen equations for frequency-dependent scattering in 2D have not been developed and so a detailed comparison for the superconducting state cannot be made; however, qualitatively the frequency-dependent scattering contribution is expected to compress the frequency range of the excess absorption in the superconducting state above the gap over that shown in Fig. 3(b). Calculations by Strassler and Fulde[15] have shown that the BCS results predict frequency compression of the optical conductivity above the gap for the Drude model in the $\omega\tau\gg 1$ limit. Although the zero-frequency spike in the conductivity shown in Fig. 2(a) is not exactly of the Drude form, it is close enough so that the same qualitative behavior can be anticipated.

The enhanced absorptivity in the superconducting state just above the gap exhibited in $La_{1.85}Sr_{0.15}CuO_{4-y}$ is explained by a combination of the grain geometry dependent coupling of a large dielectric contribution from the insulating **c** direction to the orthogonal 2D conducting planes via the composite nature of the samples, plus frequency-dependent scattering in the 2D planes. While the former will not appear in single crystals or oriented films, the latter effect will persist, providing an additional demonstration of frequency-dependent scattering. Thus the reflectivity of single crystals or oriented films of high-T_c oxides will be needed to obtain the electron-boson coupling function, $a^2F(\omega)$, unambiguously.[7]

In conclusion, we have found that (1) both La_2NiO_4 and $La_{1.85}Sr_{0.15}CuO_{4-y}$ show the same kind of electronic anisotropy, (2) the EMA with nonspherical grains provides a reasonable description of the ir and optical properties of these sintered materials, (3) the phonon modes of these structurally isomorphic systems are similar in strength and position, (4) the large value of $\epsilon_{\infty,c}$ for $La_{1.85}Sr_{0.15}CuO_{4-y}$ indicates that the electronic absorption at 0.5 eV is polarized along the **c** axis, (5) the enhanced absorption above the gap in the superconducting state is a consequence of the composite nature of the samples, along with a frequency-dependent scattering rate for the free carriers, and (6) the apparent electromagnetic gap of the sintered material depends on the grain geometry.

This work was supported by National Science Foundation Grant No. DMR-84-09823 and by the U.S. Amry Office under Grant No. DAAL03-86-K-0103. One of us (P.E.S.) was partially supported by AT&T Bell Laboratories.

[1] J. M. Bassat, P. Odier, and F. Gervais, Phys. Rev. B **35**, 7126 (1987).

[2] D. A. G. Bruggeman, Ann. Phys. (Leipzig) **24**, 636 (1935).

[3] D. C. Mattis and J. Bardeen, Phys. Rev. **111**, 412 (1958).

[4] A. S. Barker, Jr., in *Far-Infrared Properties of Solids,* edited by S. S. Mitra and S. Nudelman (Plenum, New York, 1970), p. 247.

[5] F. Gervais, P. Odier, and Y. Nigara, Solid State Commun. **56**, 371 (1985).

[6] D. Stroud, Phys. Rev. B **12**, 3368 (1975).

[7] P. E. Sulewski *et al.*, Phys. Rev. B **35**, 8829 (1987).

[8] D. A. Bonn *et al.*, Phys. Rev. B **35**, 8843 (1987).

[9] G. A. Thomas, A. J. Millis, R. N. Bhatt, R. J. Cava, and E. A. Rietman, Phys. Rev. B **36**, 736 (1987).

[10] D. A. Bonn *et al.*, Phys. Rev. Lett. **58**, 2249 (1987).

[11] G. A. Thomas *et al.*, Phys. Rev. B **36**, 846 (1987).

[12] L. Genzel *et al.*, Solid State Commun. (to be published).

[13] P. E. Sulewski *et al.*, Phys. Rev. B **36**, 2357 (1987).

[14] P. A. Lee and N. Read, Phys. Rev. Lett. **58**, 2691 (1987).

[15] M. Tinkham, in Ref. 4, p. 223.